PROCEEDINGS OF SCIENCE

PoS(ECPD2015)134

The Pellet Injector and its and Associated Diagnostics for Performing Plasma Studies on the TJ-II Stellarator

---

Kieran J. McCarthy[*,a], **N. Panadero** [a], **I. Arapoglou** [c], **S. K. Combs** [b], **J. B. O. Caughman** [b], **E. de la Cal** [a], **C. Foust** [b], **R. García** [a], **J. Hernández Sánchez** [a], **F. Martín** [a], **M. Navarro** [a], **I. Pastor** [a], **M. C. Rodríguez** [a], **J. L. Velasco** [a]

[a]*Laboratorio Nacional de Fusión, Ciemat,*
Av. Complutense 40, 28040 Madrid, Spain
[b]*Oak Ridge National Laboratory,*
Oak Ridge, Tennessee, TN 37831-6169, USA
[c]*Universidad Complutense de Madrid,*
28040 Madrid, Spain
E-mail: `kieran.mccarthy@ciemat.es`

ABSTRACT: A compact pellet injector is operating on the TJ-II stellarator. It is a four-pellet system equipped with a cryogenic refrigerator for *in-situ* hydrogen pellet formation, a fast propellant valve system for pellet acceleration (≤1200 m/s), in-line diagnostics for determining pellet velocity and mass, and injection lines to the magnetically confined plasmas ($n_e(0) \leq 5 \times 10^{19}$ m^{-3}, $T_e(0) \leq 1$ keV, $B(0) = 1$ T, average minor radius = 0.22 m) created in this heliac device. Although the primary purpose of this system is to perform plasma fuelling studies, it is well suited as an active diagnostic for studying suprathermal electron populations, magnetic field orientations, and rational surfaces. For this, optical fibre coupled silicon diodes (or avalanche photodiodes), installed outside of nearby viewports, record the Balmer Hα light (λ = 656.28 nm) emitted from the neutral cloud that surrounds a pellet as it crosses the plasma. In this way, it is possible to follow the temporal evolution of the pellet ablation. In addition, an ultrafast-frame CMOS camera, equipped with a bifurcated coherent fibre bundle, has been set-up to obtain multiple images of the neutral cloud. Finally, additional plasma diagnostics, *e.g.* Thomson Scattering, broadband bolometer arrays, Heavy Ion Beam Probes, are combined to make the overall system a very powerful tool for plasma studies.

First EPs Conference on Plasma Diagnostics - 1st ECPD
14-17 April 2015,
Villa Mondragone , Frascati (Rome) Italy

© Copyright owned by the author(s) under the terms of the Creative Commons Attribution-NonCommercial-ShareAlike Licence.

1. Introduction

Cryogenic pellets have been injected into magnetically confined plasmas for several decades [1, 2]. Although the primary purpose of such injections is to fuel the discharge, pellets can be used for other purposes such as formation of internal transport barriers or for diagnosing plasmas [3, 4]. In the latter case, the luminescence light emitted by the neutral, or partially ionized, cloud that surrounds a pellet as it traverses a plasma is collected by light sensitive detectors or imaged using cameras. Then, after analysis, the pellet ablation rate and its penetration length can be established for bench marking pellet ablation modelling, and the presence of, for instance, suprathermal electron populations can be identified and localized, cloud striations can be studied, or the local magnetic field pitch can be determined [5-7].

A compact pellet injector (PI) is now operating on the TJ-II stellarator [8]. It is a four-pellet system equipped with a cryogenic refrigerator for *in-situ* hydrogen pellet formation, fast propellant valves for pellet acceleration (800 to 1200 m/s), diagnostics for determining pellet velocity and mass [9], plus injection lines to deliver pellets to the TJ-II vacuum chamber. Although, the primary purpose of this PI is plasma fuelling, it is suited as an active diagnostic. A significant advantage of the TJ-II set-up is the optical access to the pellet path through the plasma, *i.e.*, through ports from above, behind and tangentially. In order to exploit this, light sensitive diodes and a fast-frame camera, equipped with a bifurcated coherent fibre bundle, are located outside these viewports, which together with the broad range of standard diagnostics available provide a powerful diagnostic capability [10].

2. Diagnostic set-up

When a pellet crosses the last-closed flux surface (LCFS) of the plasma, ablation of material off its surface begins and a cloud of neutral particles is created, which forms a sphere consisting of isotropic particles (μs timescale). As long as these particles remain neutral they follow the pellet with the same velocity. Then, once the cloud becomes partially ionized, the particles experience a Lorentz force that attenuates their perpendicular motion and introduces a drift of the particles. The neutral cloud also causes a self-regulating or limiting character to the ablation. It then follows the magnetic field pitch and becomes detached [2]. Moreover, the particles in the cloud are excited by collisions with plasma particles and subsequently de-excite by light emission. It is assumed that this light intensity is proportional to the ablation rate [11]. The optical diagnostics, used to monitor this light emission, and the pellet injector are summarized in the following subsections.

2.1 TJ-II stellarator

TJ-II is a four-period, low magnetic shear stellarator device with an average minor radius of ≤0.22 m and a major radius of 1.5 m [8]. It was designed to explore a wide range of rotational transforms [$0.9 \leq \iota(0)/2\pi \leq 2.2$]. Its magnetic field is generated by a system of poloidal, toroidal and vertical field coils, and the resultant cross-section of its fully 3-dimensional plasma structure is bean shaped with magnetic field $B(0) \leq 1$ T. The coil set includes 32 toroidal field (TF) coils whose centres follow a toroidal helix of radius = 1.5 m and pitch law $\theta = -4\phi$ (where θ and ϕ are poloidal and toroidal angle). The nominal coil system is completed by a central structure made up of two coils (a purely horizontal one of 3 m diameter (CC) and a helical winding (HX) wrapped around this coil that follows the same winding law as the TF coils), and a pair of circular coils (VF) carrying the same current. For this evaluation process plasmas are created and maintained using a neutral beam injector (NBI) heater that provides ≤520 kW (t_{NBI} ≤120 ms). As a result, plasmas with $n_e(0) \leq 3\times10^{19}$ m^{-3} and $T_e(0) \leq 380$ eV are achieved with a

PoS(ECPD2015)134

lithium coating on the vacuum vessel wall. Note: the electron cyclotron resonace heating system and a second NBI were both off-line for these tests.

2.2 TJ-II Pellet Injector

The PI pellet formation, acceleration, guide line diagnostics, delivery and control systems were developed, built and tested at the laboratories of the Fusion Energy Division of Oak Ridge National Laboratory, Tennessee, USA before being installed on TJ-II [9]. In TJ-II, small pellets (0.5 mm diameter (*type-1*) containing 3×10^{18} hydrogen atoms) are required for experiments in which the electron density must not rise above the gyrotron cut-off limit ($\sim1.7\times10^{19}$ m^{-3}). Note: for standard configurations the plasma volume is ~1 m^3. Larger pellets (0.66 mm (*type-2*), 0.76 mm (*type-3*) and 1 mm (*type-4*) diameter containing $\leq1.2\times10^{19}$, $\leq1.8\times10^{19}$ and $\leq4.1\times10^{19}$ H particles, respectively) are required to penetrate deep into the core of NBI heated plasmas.

A schematic of the pellet injection system is found in Fig. 1. The system consists of a gun box in which pellets are created at 10 K and a gas propellant system for pellet acceleration. Closer to TJ-II, the injection line is equipped with two diagnostics through which pellets pass before reaching TJ-II. The first consists of a light emitting diode and a light sensitive diode (light gates) to provide a time signal. The second is a microwave cavity mass detector. It provides a second timing signal whose amplitude is mass dependent thus facilitating particle accountability. In its current set-up pellet delivery is very reproducible, ($\Delta t \leq 50$ μs), with minimum mass loss due to friction because of the use of short (~2 m) straight guide tubes.

2.3 Associated Plasma Diagnostics

In order to record Balmer Hα light (λ = 656.28 nm) emitted from the neutral cloud surrounding a pellet, optical fibre based diagnostic systems have been installed outside nearby upper (TOP INNER and TOP OUTER), rear (SIDE) and tangential (TANG) optical viewports. See Fig. 1. These systems consist of a 5 m long, 600 μm diameter optical fibre (model M34L05 by Thorlabs, Newton, NJ) with a Hα filter having central wavelength of 660 nm +/-2 nm, full-width at half maximum (FWHM) of 10 +/-2 nm, and peak transmission ≥50%, (model FB660-10 by Thorlabs, Newton, NJ). The collected light is directed to the input of a switchable gain, amplified silicon photodiode detector (model PDA36A by Thorlabs, Newton, NJ). Note: lenses are not used as the acceptance angle of the fibre (with respect to pellet flight path) is ~27º FWHM which allows light to be collected along the whole pellet ablation path (≤0.4 m). For instance, for TOP OUTER, the fibre to pellet path distance varies from ~0.75 m to ~0.9 m and the light is incident on the fibre to within ~16º with respect to its normal. In the case of SIDE, the distance varies from 0.6 m to 1.05 m and the light is incident to within ~6º to the fibre normal. Next, a pellet crosses the plasma outer minor radius in ≤200 μs, so the detector bandwidth is set to a few 100's of kHz, depending on the photon flux incident on the photodiode (typically a few times 10^{12} photons/s). In this way, it is possible to follow the temporal evolution of the pellet ablation and the light emission from the neutral cloud. When increased signal bandwidth is needed (*e.g.*, high frequency signal variations, *i.e.* up to 1 MHz), the silicon detector is replaced by an avalanche photodiode (model LCSA3000-01 by Laser Components GmbH, Olching, Germany). However, in order to reduce the light reaching the detector, and thus avoid signal saturation, an appropriate neutral density filter, (*e.g.* O.D = 2.5 to 4.0), is combined with the Hα filter. Note, the amplified silicon photodiode output is $\sim2\times10^5$ V/W at 656 nm whilst the APD output is 3.6×10^8 V/W at the same wavelength. However, the use of an APD, whose gain is sensitive to changes in room temperature, results in reduced signal-to-noise ratio. Finally, for data acquisition a 12-bit, ultra high-speed multifunction board with 4 analogue inputs and 20 Msamples/s sampling rate capability is used (model PCI-DAS4020/12 by Measurement Computing Corporation, Norton, MA). It is located in a nearby PC that automatically transfers data to the TJ-II data base system.

PoS(ECPD2015)134

In order to obtain multiple images of a pellet crossing a plasma, an ultra-fast frame CMOS-camera (model APX-RS by Photron Incorp., San Diego, CA), equipped with a bifurcated coherent fibre bundle and machine-vision type camera lenses (*e.g*. model HF16SA-1 by Fujinon, Tokyo, Japan), is employed. This camera, which has 2 Gbytes of digital memory, can record between 3×10^4 (1024×1024 pixels) and 2.5×10^5 (128×16 pixels) frames per second. The electronic shutter exposure time can be controlled independently from frame rate – it can be set to ≥1 μs. Note: the exposure time can be reduced further by using an image intensifier, albeit this is not required for long exposure times due to high Hα emission from the cloud, 10^{20} to 10^{22} photons/s. The bifurcated coherent fibre bundle (custom made by Schott AG, Mainz, Germany) is 4.5 m long with a square section of 6×6 mm^2, 50 lines/mm, corresponding to 300×300 fibres. Note: transmission is >20% at 656.3 nm [12]. For viewing the pellet/plasma interaction, the bundle/lens combination is fixed to the outside of TANG, SIDE and/or TOP.

The partially ionized clouds (striations), created around the pellet as it traverses the plasma, extend along the magnetic field lines and are detached at intervals (<10 μs). These clouds can be imaged using the fast frame camera thus providing a way of visualizing material ablation along the local magnetic fields, B [13]. For the latter, at any position (R, ϕ, Z) in TJ-II, where R is major radius, ϕ is toroidal angle and Z is vertical position above the central coil, the magnetic field is defined by a vector $B = (B_r, B\phi, B_Z)$, where the subscripts indicate the radial, toroidal and vertical components, respectively. Moreover, B depends strongly on ϕ in TJ-II, unlike in a tokamak, which is very close to being axisymmetric. Now, the line-of-sight (LoS) from TANG is nearly parallel to the magnetic field lines across the plane of the pellet path (as in [17] but reversed). In contrast, the LoS from TOP, and from SIDE, are sensitive to the radial and vertical components of B, respectively. Moreover, this set-up will permit the radial and vertical components of the field lines, respectively, to be studied for comparison with studies made with Motional Stark Effect [14].

The TJ-II is equipped with a wide range of passive and active plasma diagnostics [10]. Diagnostics that are of particular interest include Thomson scattering (TS) that can provide up to two electron density and temperature profiles per discharge (with ≤500 μs separation)

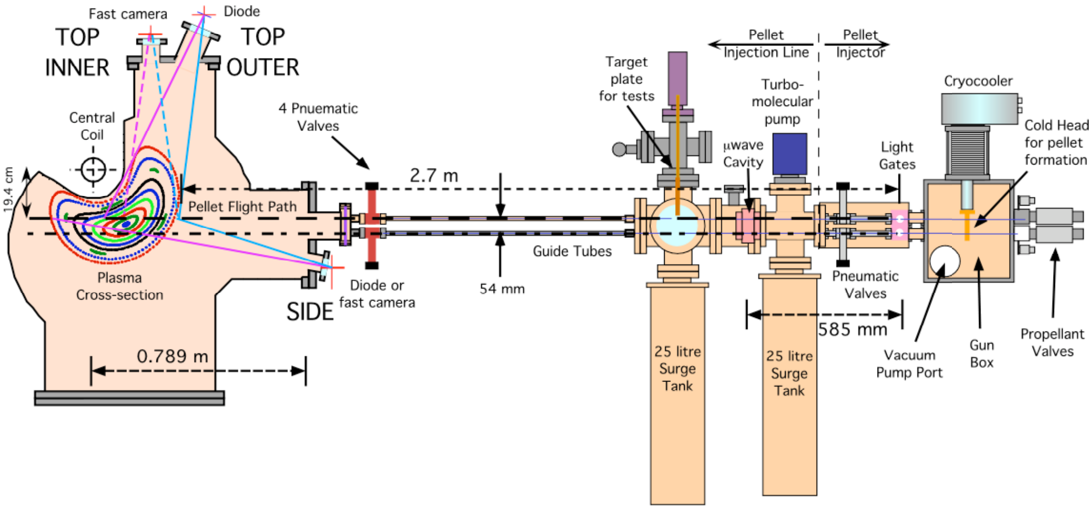

Figure 1. The TJ-II pellet injector. Left: A cross-section of the TJ-II vacuum chamber and bean-shaped plasma showing the locations and viewing directions of associated diagnostics. Right: The vacuum chamber where pellets are formed plus in-line pellet diagnostics. The flight paths for a *type*-4 and *type*-3 pellets are shown as dashed and dot-dashed black lines, respectively. *Type*-2 and *type*-1 guide tubes (not shown) are positioned above the page (with 54 mm separation from *type*-3 and -4 guide tubes, respectively). Also shown are gas surge tanks, a moveable target plate and vacuum valves.

although normally only one of each is obtained [15]. Note: the TS system is located 180º toroidally from the PI. Other diagnostics of interest include a microwave interferometer to provide the line-integrated electron density along a discharge, multiple-filter soft X-ray diagnostics to follow the temporal evolution of the core electron temperature [16], broadband bolometer arrays [17], heavy ion beam probes [18], Mirnov coil arrays to measure local magnetic field components [19], and a hard X-ray detector.

2.4 Signal analysis

In order to determine the radial location of a pellet in the plasma, time signals provided by the light gate and microwave cavity diagnostics are used. Then, knowing their separation (0.585 m) as well as the light gate to plasma edge distance, *i.e.* to the LCFS, for the magnetic configuration under study, the pellet location can be determined (assuming no acceleration). Note: the plasma minor radius varies significantly with magnetic configuration. For the standard configuration, termed 100_44_64, where the nomenclature reflects the currents in the CC, HX and VF coils (see Section 2.1), respectively, the distances from the light gate to the LCFS and from the LCFS to the centre are 2.7 m and 0.18 m, respectively for *type-4* pellets. Note: the corresponding lengths are significantly different for the other pellet types due to the 54 mm separation between guide tubes and the toroidal rotation of the magnetic configuration, *e.g.* 2.74 m and 0.172 m for *type-3* where the latter value corresponds to the distance from the plasma edge to the closest approach of the flight path to the plasma centre (See Fig. 1). Hence, Hα signals can be corrected for light collection solid angle, collection angle with respect to the fibre normal, interference filter transmission, detector efficiency and amplifier gain. Such corrections are essential to compare modelled ablation rates with Hα emission. Moreover, when imaging a pellet with the fast camera mounted either on the TOP INNER viewport or on the SIDE viewport, the pellet position is determined from the Hα signal collected by the diode mounted on the outer TOP OUTER viewport (See Fig. 1).

3. Results

An example of pellet ablation profiles in TJ-II, reconstructed from Hα signals, is plotted in Fig. 2 together with electron density profiles collected prior to, and after, injections into reproducible discharges. A good reproducibility of Hα profile shapes is apparent, as is the coherence between peaks from TOP OUTER and SIDE signals for the same pellet. However, although the agreement between the modelled ablation and Hα signal is quite good the model used still needs further adjustment [20]. For this, the TS pre-injection electron and temperature profiles of Fig. 2 b), c) were used and a 30 keV neutral beam was assumed whereas in the experiment, a 32 keV NBI with significant half and third energy components (25% and 20%, respectively) was employed. Next, the frequency of peaking in the Hα is seen to reduce after the pellet has crossed the inner most radius along its flight path. Possible explanations might be that detached ablated particles begin to rotate poloidally around the plasma centre or cold pulse propagation [22]. Such rotation is also deduced from bolometer data. In the same figure, one Hα profile exhibits a sudden increase in intensity due to a local flux of suprathermal electrons, these being induced during the ramp-up phase of this NBI-only operational mode where plasmas are generated using initial toroidal electric fields, induced by the increase of the coil currents during ramp-up, of 2.8 V and 1 V/turn. This sudden burst in light intensity indicates the total vaporization of the pellet.

The evolution of the electron density and temperature is seen in the TS profiles collected at different instances before and after pellet injection in Fig. 2 b) and c). Also shown is a representative reconstructed Hα signal. Note: reproducible plasmas were used with a target line-averaged electron density of 1.4×10^{19} m^{-3}. From these profiles, it is seen that the perturbation in temperature following pellet injection (first noted at $\rho = \sim0.5$ for $\Delta t = +136$ μs) propagates

PoS(ECPD2015)134

radially inwards and outwards faster than the rise in electron density (first noted at ρ = ~0.3 for Δt = +233 μs). The initial temperature perturbation at +136 μs also coincides with the maximum in pellet ablation (about ρ = ~0.5), and extends radially within 100 μs (the pellet radial locations at different times are indicated by the dashed vertical lines). While these test injections and results have not been full analysed as yet with relevant transport codes etc., they show the capabilities of the pellet and plasma diagnostics available in TJ-II.

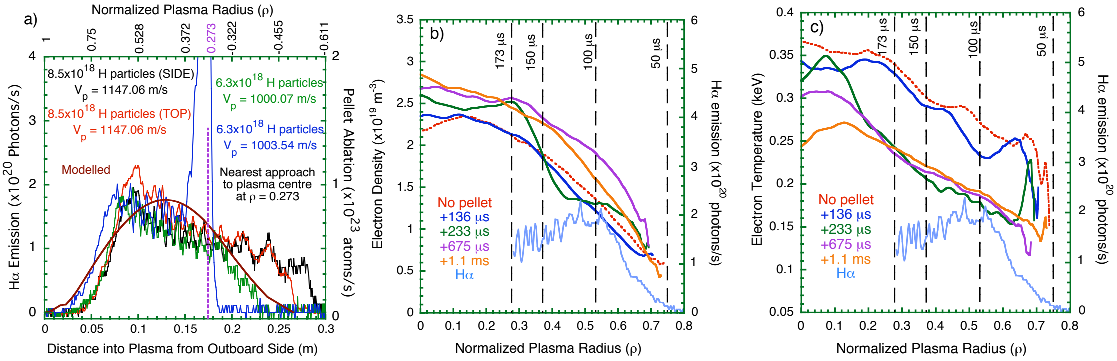

Figure 2. a) Hα light emitted by several *type*-2 pellets crossing the TJ-II plasma. TOP OUTER (red) and SIDE (black) for discharge 38054. SIDE for discharges 37984 (blue) and 38055 (green). The dashed vertical line indicates the nearest approach of *type-2* pellets to the plasma centre since their line-of-flight does not cross the plasma centre. Also shown is the modelled ablation rate (brown) for a pellet with 6.3×10^{18} particles injected at 1003 m/s. The Hα photon emission rate is estimated to be ~0.02 Hα/pellet particle/e. b) Thomson Scattering electron density profiles collected at several time instances (Δt) before and after pellet injection. All times are with respect to pellet arrival at the plasma edge. Dashed vertical lines represent pellet locations in the plasma at selected times. Also shown is a Hα signal. c) as b) but with electron temperature profiles. The TS data in b) and c) are from reproducible discharges (37982 to 37986) since the Thomson Scattering diagnostic provides a single profile per discharge. The Hα signal is from discharge 37986.

4. Conclusions

First injections of cryogenic hydrogen pellets into TJ-II plasmas have been performed and signals from some associated basic diagnostics have been processed and evaluated. These first tests indicate that the combined PI and diagnostics system will be a powerful mechanism for performing plasma fuelling experiments in TJ-II as well as a new tool for plasma studies.

Acknowledgments

This work has been carried out within the framework of the EUROfusion Consortium and has received funding from the Euratom research and training programme 2014-2018 under grant agreement No 633053. The views and opinions expressed herein do not necessarily reflect those of the European Commission. In addition, this work is partially financed by a grant from the Spanish Ministerio de Ciencia y Innovación (Ref. ENE2013-48679-R).

References

[1] S. L. Milora, W. A. Houlbergg, L. L. Lengyel and V. Mertens, *Pellet fuelling*, Nucl. Fusion 35 (1995) 657.

[2] B. Pégourié, *Pellet injection experiments and modelling,* Plasma Phys. Control. Fusion 49 (2007) R87.

PoS(ECPD2015)134

[3] L. R. Baylor et al., *Improved core fuelling with high field side pellet injection in the DIII-D tokamak*, Phys. Plasmas 7 (2000) 1878.

[4] P. Klaywittaphat et al., *Formation of internal transport barrier in tokamak triggered by pellet injection*, in proceedings of *41st EPS Conference on Plasma Physics*, June, 23 - 27, 2014 Berlin, Germany,

[5] S. L. Milora, et al., *Results of hydrogen pellet injection into ISX-B*, Nucl. Fusion 20 (1980) 1491.

[6] H. W. Muller et al., *Improvement of q-profile measurement by fast observation of pellet ablation at ASEDX Upgrade*, Rev. Sci. Instrum. 68 (1997) 4051.

[7] J. Baldzuhn et al., *Penetration studies for deuterium pellets in Wendelstein 7-AS*, Fusion Sci. Tech. 46 (2004) 348.

[8] J. Sánchez et al., *Overview of TJ-II experiments*, Nucl. Fusion 51 (2011) 094022.

[9] S. K. Combs et al., *Results from laboratory testing of a new four-barrel pellet injector for the TJ-II stellarator,* Fusion Sci. Tech. 64 (2013) 513.

[10] K. J. McCarthy et al. Proc. XXXIII Reunión Bienal de la Real Sociedad Española de Física, Santander Spain, Part IV (PUbliCan, Santander, 2011), pp. 65-67.

[11] D. H. McNeill, *H-alpha photon yield in fuelling of tokamaks*, J. Nucl. Mat. 162-164 (1989) 476.

[12] E. de la Cal et al., *The visible intensified cameras for plasma imaging in the TJ-II stellarator*, Contrib. Plasma Phys. 51 (2010) 742.

[13] R. Sakamoto et al., *Observation of pellet ablation behaviour on the Large Helical Device*, Nucl. Fusion 44 (2004) 24.

[14] K. J. McCarthy et al., *A spectrally resolved Motional Stark Effect diagnostics for the TJ-II stellarator,* Contrib. Plasma Phys. 55 (2015).

[15] J. Herranz, F. Castejón, I. Pastor and K. J. McCarthy, *The spectrometer of the high-resolution multiposition Thomson scattering diagnostic for TJ-II*, Fusion Eng. and Design 65 (2003) 525.

[16] D. Baiao, et al., *Implementation of a multichannel soft x-ray diagnostic for electron temperature measurements in TJ-II high density plasmas*, Rev. Sci. Instrum. 83 (2012) 10E104.

[17] M. A. Ochando, et al., *Up-down and in-out asymmetry monitoring based on broadband radiation detectors*, Fusion Sci. Tech. 50 (2006) 313.

[18] A. V. Melnikov et al., *Plasma potential evolution study by HIBP diagnostic during NBI experiments in the TJ-II stellarator*, Fusion Sci. Tech. 51 (2007) 31.

[19] R. Jiménez-Gómez, et al., *Analysis of magnetohydrodynamic instabilities in TJ-II plasmas*, Fusion Sci. Tech. 51 (2007) 20.

[20] Y. Nakamura et al., *An analysis of the ablation rate for solid pellets injected into neutral beam heated toroidal plasmas*, Nucl. Fusion 26 (1986) 907.

[21] S. Sudo el al., *Recent diagnostic developments on LHD*, Plasma Phys. Control. Fusion (2003) A425.